Nanoscale

PAPER

View Article Online
View Journal | View Issue

Cite this: *Nanoscale*, 2021, **13**, 2465

DNA modification and visualization on an origami-based enzyme nano-factory†

Elmar Weinhold [a] and Banani Chakraborty *[b]

Received 23rd October 2020,
Accepted 18th December 2020

DOI: 10.1039/d0nr07618j

rsc.li/nanoscale

The past decade has seen enormous progress in DNA nanotechnology through the advent of DNA origami. Functionalizing the DNA origami for multiple applications is the recent focus of this field. Here we have constructed a novel DNA enzyme nano-factory, which modifies target DNA embedded on a DNA origami platform. The enzyme is programmed to reside in close proximity to the target DNA which enhances significantly the local concentration compared to solution-based DNA modification. To demonstrate this we have immobilized DNA methyltransferase M·TaqI next to the target DNA on the DNA origami and used this enzyme to sequence-specifically modify the target DNA with biotin using a cofactor analogue. Streptavidin binding to biotin is applied as a topographic marker to follow the machine cycle of this enzyme nano-factory using atomic force microscopy imaging. The nano-factory is demonstrated to be recyclable and holds the potential to be expanded to a multi-enzyme, multi-substrate operating system controlled by simple to complex molecules made of DNA, RNA or proteins.

Introduction

Progress in structural DNA nanotechnology[1a,b] has taken a huge leap, especially in the last decade, upon the introduction of DNA origami.[2a,b] Recently, DNA origami research has shifted its gear from structural hierarchy[3a–e] to functional intricacy.[4a,b] Precise structural modification to functionalize the origami[5a–g] has opened new dimensions to solve existing problems in cargo delivery,[6a–c] observing single molecule integration[7a,b] on bio-surfaces, targeting various guests through orientation of hosts[8a–f] on one platform and beyond.[9a–f] Protein assemblies on DNA origami have been studied for various enzymatic activities by single and multiple embedded proteins.[10a–g] Here we show that the origami platform can host both DNA-modifying enzyme and its target DNA for enzymatic activity and build an enzyme nano-factory using bio-molecular interactions. We have chosen DNA methyltransferase (MTase) M·TaqI which can modify the double-stranded 5′-TCGA-3′ sequence with various chemical groups using natural and synthetic cofactors.[11a–c] M·TaqI was conjugated with an oligodeoxynucleotide (ODN) for hybridization with a complementary docking strand on the origami. Conjugation was performed by maleimide chemistry using an M·TaqI single cysteine mutant, in which the internal cysteine at position 48 was replaced by serine (C48S) and an additional cysteine residue was added to the C-terminal end (422C). This double mutant was then covalently linked to maleimide-modified ODN without hampering the active site of the enzyme. In addition, the DNA substrate containing the recognition sequence was placed next to M·TaqI. We have chosen a biotinylated aziridine cofactor (6BAz)[12] to couple biotin to the target DNA sequence by the DNA MTase, so that biotin can further interact with streptavidin and hence can be used as a topographic marker for tracking the efficiency of the enzyme nano-factory by atomic force microscopy (AFM).

Schematic representation of the enzyme nano-factory and its machine cycle is shown in Fig. 1. Rectangular origami

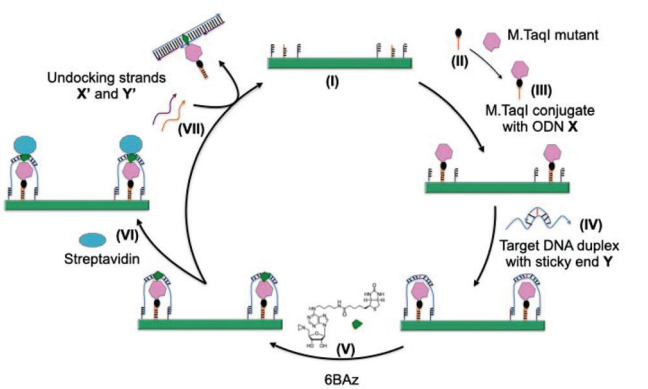

Fig. 1 Schematic flow of the machine cycle for the enzyme nano-factory and product detection after the addition of streptavidin.

[a]*Institute of Organic Chemistry, RWTH Aachen University, Landoltweg 1, 52056 Aachen, Germany*
[b]*Department of Chemical Engineering, Indian Institute of Science, Bangalore 560012, India. E-mail: banani@iisc.ac.in*

†Electronic supplementary information (ESI) available. See DOI: 10.1039/d0nr07618j

shown in green is modified with orange docking strands to hybridize partially with M·TaqI double mutant (shown in pink) conjugated with ODN (**X**, orange). The DNA origami surface has 4 binding positions for the M·TaqI-ODN conjugate (as shown in Fig. S1†) but only 2 out of 4 are shown in the schematics for simplicity (side view). In the next step target DNA with a partial complementary sequence (**Y**) is hybridized with the black docking strands in close proximity to the M·TaqI-ODN docking site. Target DNA modification with biotin by enzymatic modification with the 6BAz cofactor is represented with a green shape. Upon the addition of streptavidin (topographic marker), biotin–streptavidin complexes can be detected by a height marker of 5 nm next to the M·TaqI-ODN conjugate (which also is 5 nm high). They are expected to look like 'twin-spots' of 5 nm height next to each other. Finally, addition of undocking strands fully complementary to the target DNA (**Y′**) and M·TaqI-ODN conjugate (**X′**) removes the modified DNA product and M·TaqI-ODN to regenerate the origami surface through branch migration.

Results & discussion

The formation of rectangular DNA origami as programmed by CaDNAno[13] is shown in Fig. 2a. Spots on the DNA origami are observed for bound M·TaqI-ODN conjugates in 1, 2, 3 or 4 out of 4 programmed positions as pointed by white arrows in the 5 nm height profile and yellow arrows in the 10 nm height profile (Fig. 2b). After complete addition of all components required for the modification and visualization two closely located spots (twin-spots) are detected on the programmed positions on the origami surface. Fig. 2c shows AFM images of both 5 nm and 10 nm height profiles. White double arrows indicate the 5 nm twin-spots in 5 nm max. height profile and yellow arrow pairs point to the twin-spots in 10 nm max. height profiles. One spot originates from bound M·TaqI-ODN conjugates and the other spot results from the topographically marked modification product resulting from streptavidin binding to successfully biotinylated target DNA. Observation of twin-spots is expected due to the flexibility of the two surface-bound proteins. Fig. 2d shows the AFM images for completing a full nano-factory cycle after removal of the products from the origami platform. The twin-spots are removed using fully complementary DNA strands **X′** and **Y′** to release the DNA product and enzyme and regenerate the rectangular origami surface. Fig. 2e shows a control experiment where M·TaqI was not covalently conjugated with ODN and hence not embedded in the origami surface. Here we do not see any 5 nm spots on the DNA origami indicating that the origami-bound target DNA is not modified by free M·TaqI at a low nM concentration, while keeping all other experimental conditions the same. A comparable result is obtained in the absence of the M·TaqI-ODN conjugate (Fig. 2f). Fig. 2g shows that there are no twin-spots when the 6BAz cofactor is missing. Only 5 nm spots resulting from origami-bound M·TaqI-ODN conjugates are visible.

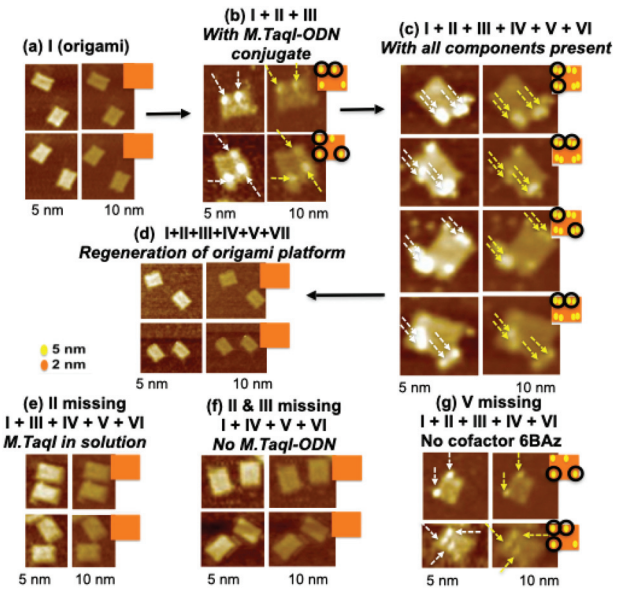

Fig. 2 AFM images of stepwise operation of a complete enzyme nano-factory cycle: (a) origami platform (I) only; (b) upon addition of the M·TaqI-ODN conjugate (II + III); (c) upon addition of the M·TaqI-ODN conjugate (II + III), target DNA (IV), 6BAz cofactor (V) and streptavidin (VI); (d) upon addition of the M·TaqI-ODN conjugate (II + III), target DNA (IV), 6BAz cofactor (V), undocking strands X′ and Y′ (VII). Control experiments: (e) M·TaqI is not embedded on the origami surface but free in solution; (f) M·TaqI and conjugated DNA both are missing; (g) cofactor 6BAz is missing. Schematic drawings next to AFM images show the expected height profile in (a)–(g). Schematic height profiles are shown with color coding, orange 2 nm; yellow 5 nm height and spots observed on individual origami are encircled.

Statistics as described in Table 1 shows that 69% of the four programmed reaction centers on each origami surface are occupied by the M·TaqI-ODN conjugate and 54% of them lead to a modified product on the surface. This gives an overall

Table 1 Calculated efficiency of the enzyme nano-factory

Total origami counted	Theoretical maximum of M·TaqI (max. 4 in each origami)	Total M·TaqI modificaion counted	Total streptavidin modification counted	Percentage of M·TaqI modification observed	Percentage of streptavidin modification observed	Overall percentage of streptavidin modification observed
50	200	138	75	69%	54%	37%

37% yield of conversion if all programmed positions are regarded. Additional representative AFM images are shown in Fig. S5† based on which the yields in Table 1 are calculated. The absence of twin-spots is considered as failed modification. However, these experiments will not report at which point the modification failed. It could just be that the target DNA is not present on the origami surface or one or more of the other factors are missing on a particular reaction centre. However, if we define only at least one twin-spot *per* origami as successful modification, this enzyme nano-factory will show a much higher yield. The enzyme nano-factory was designed to bring the target DNA in close proximity to M·TaqI by doubly anchoring the target DNA on the origami. Our assumption was to reduce the flexibility of the target DNA in the vicinity of the enzyme active site to enhance the modification yield. In this particular work, our plan was to maximise the yield of modification and hence we did not investigate whether a singly anchored target DNA will work as well. For a more dynamic system the modification yield could be tuned by muting one or the other anchor.

The lower yield on the surface compared to almost quantitative modification when both M·TaqI and target duplex are in solution (Fig. S4†), can not only be attributed to a slower enzymatic reaction caused by the shorter incubation time, lower temperature, lower cofactor concentration and different buffers but also to two additional steps on the surface: first, hybridization of the M·TaqI-ODN conjugate to the origami is only 69%. Higher ratios of the conjugate to origami lead to improved yields but the AFM quality of visualization became poor. Second, the last step of streptavidin addition also had to be optimized to achieve the best possible visualisation and higher concentrations of streptavidin (above 2 μM) or longer incubation times (more than 3–5 min) resulted in non-specific deposition of the protein to the surface. Thus, keeping the conditions below saturation, we have been able to prove successfully that the M·TaqI nano-factory is able to modify target DNA on the origami surface with biotin at precisely programmed positions with the enzyme placed in near proximity to the substrate. However the statistical count can be regarded as a minimal efficiency of this enzyme nano-factory performance because it is optimized for best visualisation by AFM without protein crowding on the surface. With streptavidin nano-gold and visualization through TEM, which is independent of the topographic marker crowding, a more sensitive and quantitative analysis could be possible. In addition, the advantage of this generic origami platform is that the product can be removed to regenerate the surface for the next set of enzymatic operations. In consecutive cycles various target DNA sequences for different DNA-modifying enzymes could be used to modify target DNA with various cofactors and finally observed with different visual markers. This can be viewed as a prototype for a multi-component device which can be logically programmed to be applied in various nano-devices.

Experimental section

Design, preparation and purification of rectangular DNA origami

Rectangular DNA origami with a length of 92 nm and width of 52 nm was designed using CaDNAno[13] software. This rectangular origami (Fig. S1†) has four positions with elongated staple strands (docking strands shown in orange in Fig. 1a) to hybridise with DNA **X** conjugated with M·TaqI (double mutant) and four neighbouring pairs of elongated staple strands (docking strands shown in purple in Fig. 1a) to hybridise with partial DNA duplexes containing a target sequence of M·TaqI and sticky ends **Y**. The designed 221 short DNA staple strands, which help to fold the single-stranded M13mp18 viral plasmid DNA in a rectangular shape, and the MTase-binding DNA **X**, target DNA duplex **Y** and undocking DNA strands for the release of M·TaqI (**X′**) and target DNA duplex (**Y′**) were ordered from Sigma Aldrich, Germany. M13mp18 (0.4 nM) was mixed with staple strands (20 nM) and docking strands (80 nM) in origami buffer (40 mM Tris-HCl, 2 mM acetic acid, 2.5 mM EDTA, 12.5 mM $Mg(OAc)_2$, pH 8.0). Origami samples (typical 25–50 μL) were annealed in PCR tubes using an Eppendorf PCR cycler with a two step cooling gradient: from 90 °C to 60 °C at a cooling rate of 2.36 min per °C and from 60 °C to 16 °C at a cooling rate of 16.36 min per °C and then at 16 °C for a minimum of 30 min. Furthermore, the DNA origami samples are purified with Millipore Microcon 50 kDa spin columns with a speed of 14 000 rpm for 2–3 min and washed with origami buffer to remove excess of staple strands.

Design, preparation and purification of the M·TaqI double mutant

M·TaqI was mutated at two positions to assure that thiolated amino acid cysteine is present only at the C-terminal position for coupling with maleimide-modified ODN. Hence the single cysteine residue at position 48 was mutated to a serine residue and one extra cysteine was added at the C-terminal end (the 422nd position). M·TaqI C48S422C was expressed in *E. coli* and purified by cation exchange chromatography with salt gradient, concentrated using ultrafiltration upon centrifugation and further purified by size exclusion chromatography. Wild

type M·TaqI was also purified using the same procedure[14] and used for control experiments. Both enzyme preparations are protected from oxidation (dimerisation) using β-mercaptoethanol. SDS-PAGE was used to analyse the purity of M·TaqI C48S422C (Fig. S2a and S2b†). Less than 5% dimerisation was observed in the gel, which ensures that the enzyme was ready to be modified for immobilisation on the origami surface.

Activity test of M·TaqI

The M·TaqI double mutant is expected to methylate λ DNA within the double stranded 5′-TCGA-3′ target sequences and once methylated those sequences are protected against fragmentation by the cognate restriction endonuclease R·TaqI. We have performed such a modification-restriction assay by incubating decreasing amounts of M·TaqI double mutant ranging from 10 ng to 20 pg (9 two-fold serial dilutions) with a constant amount of λ DNA (0.05 ng μL^{-1}) and natural cofactor *S*-adenosyl-L-methionine (80 μM) at 65 °C for 1 h followed by the addition of R·TaqI. Agarose gel (1%) electrophoresis was performed at 100 V for 40 min to analyse the degree of DNA protection. Results from this activity assay are shown in Fig. S2c.† It confirms that even sub-nanogram amounts of the M·TaqI double mutant are enough to fully protect λ DNA (full protection including lane 6) and this activity is very similar to the activity of the wild type enzyme.[18]

Conjugation of M·TaqI double mutant with NH_2-modified-ODN (X)

NH_2-modified-ODN (20 μM, 5′-NH_2-CGA CGA TAA GTC-3′, **X**) was incubated with hetero-bifunctional crosslinker *N*-(γ-maleimidobutyryloxy)succinimide (GMBS) (4 mM) at room temperature for 2 h in a buffer consisting of 100 mM NaH_2PO_4, 150 mM NaCl, 30% DMF at pH 7.4 (Fig. S3a†). The GMBS-modified ODN was purified by reverse-phase HPLC. The purified product was further incubated with M·TaqI double mutant at 4 °C for 1 h in conjugation buffer made of 4.3 mM Na_2HPO_4, 1.4 mM K_2HPO_4, 140 mM NaCl, 2.7 mM KCl, and 0.01% Triton X-100 at pH 7.2. The formation of the M·TaqI-ODN conjugate was verified by SDS-PAGE. Electrophoresis was performed at room temperature and 200 V for 1.5 h with 10 pmol M·TaqI double mutant (Fig. S3b†). Over 50% conversion to the conjugate with lower mobility was observed with stoichiometric amounts of both reaction partners (1 : 1) and could be increased to about 70% applying a 10-fold excess of GMBS-modified ODN (1 : 10).

Modification of target DNA with biotinylated cofactor 6BAz in solution

The modification of target DNA with synthetic cofactor 6BAz was demonstrated in solution using M·TaqI (wild type) with a 14 base pair hemi-methylated duplex DNA (5′-GCC GAT CGA TGC CG-3′//5′-CGG CAT CGA(Me) TCG GC-3′, M·TaqI recognition sequence underlined). The DNA duplex was pre-annealed in reaction buffer (20 mM Tris-HOAc, 50 mM KOAc, 10 mM $Mg(OAc)_2$, pH 6.0) by incubation at 95 °C for 2 min and cooling to room temperature for 15 min. The modification reaction was performed with target DNA (10 μM), M·TaqI (11 μM), 6BAz (80 μM) and incubation overnight at 37 °C. Half of the SMILING[10] reaction mixture was further incubated with Proteinase K (3 mAu) at 37 °C for 1 h to fragment the DNA MTase and release the modified duplex. Non-denaturing polyacrylamide gel (15%) electrophoresis was performed with 10 pmol samples at room temperature at 130 V for 1 h. The gel was stained with GelRed in NaCl solution (0.1 mM) for 5 min and visualisation of bands was done under UV irradiation (312 nm). Fig. S4† shows the gel result of target DNA modification with 6BAz using M·TaqI. The formation of a low mobility band in lane 3 is almost quantitative and attributed to the very stable complex between M·TaqI and 6BAz-modified DNA. Lane 4 shows that upon treatment with Proteinase K the modified DNA runs with almost similar mobility as the unmodified target DNA. A slightly slower mobility can be attributed to the covalent biotin modification.

Operation of the nano-enzyme-factory

Experimental details for running the entire DNA-enzyme nano-factory, which is schematically depicted in Fig. 1, is tabulated stepwise in Table S1.† The M·TaqI double mutant (800 nM) was conjugated with GMBS-modified ODN (800 nM) in conjugation buffer for 1 h at 4 °C, added to pre-formed origami (0.4 nM) and incubated at 4 °C overnight. Pre-annealed target DNA (800 nM) was added to the origami-enzyme complex and incubated again at 4 °C overnight. 6BAz (2 μM) was added to the mixture above and incubation continued for 2 h. The sample (5 μL) was deposited on freshly cleaved mica surface for 5 min, washed with origami buffer (5 times 50 μL) and dried. Streptavidin (2 μM) was dropcast on the mica surface for 5 min followed by washing with origami buffer (5 times 50 μL), drying and observation under AFM. Washing, drying and observation were repeated up to 4 times to optimise quality of the AFM pictures. In addition, samples were observed under AFM after completion of various steps and in the absence of various components as illustrated in Fig. 2.

Reversibility test of the enzyme nano-factory

To make this nano factory fully reversible we programmed to remove the modified biotinylated target DNA and the M·TaqI-ODN conjugate by adding undocking strands **X′** and **Y′** (8 μM each) and incubation at 4 °C overnight. Surface regeneration was verified by AFM.

Atomic force microscopy (AFM) visualisation

Imaging was performed with a Digital Instrument Nanoscope IIIA Multimode AFM. The AFM was operated in the tapping in air mode with a silicon nitride tip from Nano World Pointprobe. Several 512 × 512 pixel AFM images were recorded from separate locations across the mica surfaces to ensure reproducibility of the results. All images were analysed using Nanoscope software. AFM images were obtained after PCR annealing and micro-filtration of origami samples [t = 24 h], after hybridization of the M·TaqI mutant conjugated DNA and target DNA with the DNA origami [t = 48 h], after adding the

6BAz cofactor [t = 50 h], after adding the topographic marker streptavidin on the surface [t = 51 h] and finally after adding undocking strands [t = 74 h].

Conclusions

We have successfully demonstrated the first cycle of an enzyme nano-factory on a DNA origami surface. A double mutant of M·TaqI is specifically conjugated with an ODN for attaching the enzyme on the origami surface and modifying nearby bound target DNA with biotin in the presence of a cofactor analogue. Finally streptavidin is used as a topographic marker to track the progress and efficiency of the enzyme nano-factory using AFM. We have shown when M·TaqI on the nano-factory successfully modifies target DNA on the origami surface, it is very uniquely marked by twin-spots of 5 nm height or with up to 10 nm height spots. Omitting any component resulted in the absence of such topographic signatures. Another unique feature of this nano-factory is that it is being run on a DNA-based platform (origami), DNA is the target and DNA strands are used for product removal and recycling. Coupling multiple of such controlled nano-devices one can imagine to design much more complex circuits which can mimic some of the fascinating systems in biology. This work holds promise to be extended on DNA-nano-biochip platforms[15] to design and demonstrate complex yet parallel biosensors for parallel target screening.[16] Even further one can incorporate such devices to control *in vivo* drug delivery machineries using DNA origami packaging technology.[17]

Conflicts of interest

The manuscript was written through contributions of both authors. All authors have given approval to the final version of the manuscript. There are no conflicts to declare.

Acknowledgements

B. C. thanks Alexander von Humboldt Foundation, Germany, for postdoctoral fellowship at the RWTH Aachen University, Germany, and DBT Ramalingaswami Fellowship from the Department of Biotechnology, Government of India. We thank Kerstin Glensk for preparing M·TaqI C48S422C and Prof. Ulrich Simon, RWTH Aachen University, Germany, for using Atomic Force Microscopy to acquire the images shown in this work. B. C. also thanks Prof Nadrian C. Seeman for meaningful discussion and guidance.

References

1 (*a*) N. C. Seeman, Structural DNA Nanotechnology: Growing Along with Nano Letters, *Nano Lett.*, 2010, **10**, 1971–1978; (*b*) H. Li, J. D. Carter and T. H. LaBean, Nanofabrication by DNA self-assembly, *Mater. Today*, 2009, **12**, 24–32.

2 (*a*) P. W. K. Rothemund, Folding DNA to create nanoscale shapes and patterns, *Nature*, 2006, **440**, 297–302; (*b*) B. Sacca and C. Niemeyer, DNA origami: the art of folding DNA, *Angew. Chem., Int. Ed.*, 2012, **51**, 58–66.

3 (*a*) T. Torring, N. V. Voigt, J. Nangreave, H. Yan and K. V. Guthelf, DNA origami: a quantum leap for self-assembly of complex structures, *Chem. Soc. Rev.*, 2011, **40**, 5636–5646; (*b*) Y. Ke, L. L. Ong, W. M. Shih and P. Ying, Three-dimensional structures self-assembled from DNA bricks, *Science*, 2013, **338**, 1177–1183; (*c*) E. Benson, A. Mohammed, J. Gardell, S. Masich, E. Czeizler, P. Orponen and B. Högberg, DNA rendering of polyhedral meshes at the nanoscale, *Nature*, 2015, **523**, 441–444; (*d*) C. E. Castro, F. Kilchherr, D.-N. Kim, E. L. Shiao, T. Wauer, P. Wortmann, M. Bathe and H. Deitz, A primer to scaffolded DNA origami, *Nat. Methods*, 2011, **8**, 221–229; (*e*) S. M. Douglas, H. Dietz, T. Liedl, B. Högberg, F. Graf and W. M. Shih, Self-assembly of DNA into nanoscale three-dimensional shapes, *Nature*, 2009, **459**, 414–418.

4 (*a*) B. Sacca and C. M. Niemeyer, Functionalization of DNA nanostructures with proteins, *Chem. Soc. Rev.*, 2011, **40**, 5910–5921; (*b*) K. Jahn, T. Tørring, N. V. Voigt, R. S. Sørenson, A. L. B. Kodal, E. S. Anderson, K. V. Gothelf and J. Kjems, Functional patterning of DNA origami by parallel enzymatic modification, *Bioconjugate Chem.*, 2011, **22**, 819–823.

5 (*a*) A. Kuzuya, M. Kimura, K. Numajiri, N. Koshi, T. Ohnishi, F. Okada and M. Komiyama, Precisely programmed and robust 2D streptavidin nanoarrays by using periodical nanometer–scale wells embedded in DNA origami assembly, *ChemBioChem*, 2009, **10**, 1811–1815; (*b*) R. Subramani, S. Juul, A. Rotaru, F. F. Anderson, K. V. Gothelf, W. Mamdouh, F. Besenbacher, M. Dong and B. R. Knudsen, A novel secondary DNA binding site in human topoisomerase I unravelled by using a 2D DNA origami platform, *ACS Nano*, 2010, **4**, 5969–5977; (*c*) Y. Yang, Y. Liu and H. Yan, DNA nanostructures as programmable biomolecular scaffolds, *Bioconjugate Chem.*, 2015, **26**, 1381–1395; (*d*) C. Timm and C. M. Niemeyer, Assembly and Purification of Enzyme–Functionalized DNA Origami Structures, *Angew. Chem., Int. Ed.*, 2015, **54**, 6745–6750; (*e*) R. Meyer and C. M. Niemeyer, Orthogonal protein decoration of DNA nanostructures, *Small*, 2011, **22**, 3211–3218; (*f*) R. Chhabra, J. Sharma, Y. Ke, Y. Liu, S. Rinker, S. Lindsay and H. Yan, Spatially addressable multiprotein nanoarrays templated by aptamer-tagged DNA nanoarchitectures, *J. Am. Chem. Soc.*, 2007, **129**, 10304–10305; (*g*) N. D. Derr, B. S. Goodman, R. Jungmann, L. E. Leschziner, W. M. Shih and S. L. Reck-Peterson, Tug-of-war in motor protein ensembles revealed with a programmable DNA origami scaffold, *Science*, 2012, **338**, 662–665.

6 (*a*) Q. Zhang, Q. Jiang, N. Li, L. Dai, Q. Liu, L. Song, J. Wang, Y. Li, J. Tian, B. Ding and Y. Du, DNA Origami

as an In Vivo Drug Delivery Vehicle for Cancer Therapy, *ACS Nano*, 2014, **8**, 6633–6643; (*b*) A. S. Walsh, H. Yin, C. M. Erben, M. J. A. Wood and A. J. Turberfield, DNA cage delivery to mammalian cells, *ACS Nano*, 2011, **5**, 5427–5432; (*c*) Q. Jiang, Y. Shi, Q. Zhang, N. Li, P. Zhan, L. Song, L. Dai, J. Tian, Y. Du, Z. Chen and B. Ding, A self–assembled DNA origami–gold nanorod complex for cancer theranostics, *Small*, 2015, **11**, 5134–5141.

7 (*a*) A. Rajendran, M. Endo and H. Sugiyama, Single–Molecule Analysis Using DNA Origami, *Angew. Chem., Int. Ed.*, 2012, **51**, 874–890; (*b*) N. Stephanopoulos, M. Liu, G. J. Tong, Z. Li, Y. Liu, H. Yan and M. B. Francis, Immobilization and one-dimensional arrangement of virus capsids with nanoscale precision using DNA origami, *Nano Lett.*, 2010, **10**, 2714–2720.

8 (*a*) F. Diezmann and O. Seitz, DNA-guided display of proteins and protein ligands for the interrogation of biology, *Chem. Soc. Rev.*, 2011, **40**, 5789–5801; (*b*) J. Fu, M. Liu, Y. Liu, N. W. Woodbury and H. Yan, Interenzyme Substrate Diffusion for an Enzyme Cascade Organized on Spatially Addressable DNA Nanostructures, *J. Am. Chem. Soc.*, 2012, **134**, 5516–5519; (*c*) J. Fu, Y. R. Yang, A. Johnson-Buck, M. Liu, Y. Liu, N. G. Walter, N. W. Woodbury and H. Yan, Multi-enzyme complexes on DNA scaffolds capable of substrate channelling with an artificial swinging arm, *Nat. Nanotechnol.*, 2014, **9**, 531–536; (*d*) E. Kazenwadel, M. Franzreb and B. E. Rapp, Synthetic enzyme supercomplexes: co-immobilization of enzyme cascades, *Anal. Methods*, 2015, **7**, 4030–4037; (*e*) J. Fu, Y. R. Yang, S. Dhakal, Z. Zhao, M. Liu, T. Zhang, N. G. Walter and H. Yan, Assembly of multienzyme complexes on DNA nanostructures, *Nat. Protoc.*, 2012, **11**, 2243–2273; (*f*) F. Simmel, DNA-based assembly lines and nanofactories, *Curr. Opin. Biotechnol.*, 2012, **23**, 516–521.

9 (*a*) Y. Fu, D. Zeng, J. Chao, Y. Jin, Z. Zhang, H. Liu, D. Li, H. Ma, Q. Huang, K. V. Gothelf and C. Fan, Single-step rapid assembly of DNA origami nanostructures for addressable nanoscale bioreactors, *J. Am. Chem. Soc.*, 2013, **135**, 696–702; (*b*) C. Lin, Y. Liu and H. Yan, Designer DNA nanoarchitectures, *Biochemistry*, 2009, **48**, 1663–1674; (*c*) F. Zhang, J. Nangreave, Y. Liu and H. Yan, Structural DNA nanotechnology: state of the art and future perspective, *J. Am. Chem. Soc.*, 2014, **136**, 11198–11211; (*d*) A. Chopra, S. Krishnan and F. Simmel, Electrotransfection of polyamine folded DNA origami structures, *Nano Lett.*, 2016, **16**, 6683–6690; (*e*) M. Endo, Y. Yang and H. Sugiyama, DNA origami technology for biomaterials applications, *Biomater. Sci.*, 2013, **1**, 347–360; (*f*) V. Kumar, S. Pallazzolo, S. Bayda, G. Corona, G. Toffoli, F. Toffoli and F. Rizzolio, DNA nanotechnology for cancer therapy, *Theranostics*, 2016, **6**, 710–725.

10 (*a*) W. P. Klein, R. P. Thomsen, K. B. Turner, S. A. Walper, J. Vranish, J. Kjems, M. G. Ancona and I. L. Medintz, Enhanced catalysis from multienzyme cascades assembled on a DNA origami triangle, *ACS Nano*, 2019, **13**, 13677–13689; (*b*) Y. Xu, Y. Gao, Y. Su, L. Sun, F. F. Xing, C. Fan and D. Li, Polydopamine nanosphere@ silver nanoclusters for fluorescence detection of multiplex tumor markers, *J. Phys. Chem. Lett.*, 2018, **9**, 6786–6794; (*c*) K. Zhou, Y. Ke and Q. Wang, Selective in situ assembly of viral protein onto DNA origami, *J. Am. Chem. Soc.*, 2018, **140**, 8074–8077; (*d*) S. Li, Q. Jiang, S. Liu, Y. Zhang, Y. Tian, C. Song, J. Wang, Y. Zou, G. J. Anderson, J.-Y. Han, Y. Chang, Y. Liu, C. Zhang, L. Chen, G. Zhou, G. Nie, H. Yan, B. Ding and Y. Zhao, A DNA nanorobot functions as a cancer therapeutic in response to a molecular trigger in vivo, *Nat. Biotechnol.*, 2018, **36**, 258–264; (*e*) Y. Chen, G. Ke, Y. Ma, Z. Zhu, M. Liu, Y. Liu, H. Yan and C. J. Yang, A synthetic light-driven substrate channeling system for precise positioning of enzyme, cascade activity based on DNA origami, *J. Am. Chem. Soc.*, 2018, **140**, 8990–8996; (*f*) Y. R. Yang, J. Fu, S. Wootten, X. Qi, M. Liu, H. Yan and Y. Liu, 2D enzyme cascade network with efficient substrate channeling by swinging arms, *ChemBioChem*, 2018, **19**, 212–216; (*g*) J. Fu, Y. R. Yang, S. Dhakal, Z. Zhao, M. Liu, T. Zhang, N. G. Walter and H. Yan, Assembly of multienzyme complexes on DNA nanostructures, *Nat. Protoc.*, 2016, **11**, 2243–2273.

11 (*a*) G. Pljevaljčić, F. Schmidt and E. Weinhold, Sequence–specific methyltransferase–induced labeling of DNA (SMILing DNA), *ChemBioChem*, 2004, **5**, 265–269; (*b*) G. Pljevaljcic, F. Schmidt, A. J. Scheidig, R. Lurz and E. Weinhold, Quantitative labeling of long plasmid DNA with nanometer precision, *ChemBioChem*, 2007, **8**, 1516–1519; (*c*) S. Klimasauskas and E. Weinhold, A new tool for biotechnology: AdoMet-dependent methyltransferases, *Trends Biotechnol.*, 2007, **25**, 99–104.

12 (*a*) S. Wilkinson, M. Diechtierow, R. A. Estabrook, F. Schmidt, M. Hüben, E. Weinhold and N. O. Reich, Enzyme-directed positioning of nanoparticles on large DNA templates, *Bioconjugate Chem.*, 2008, **19**, 470–475; (*b*) G. Braun, M. Diechtierow, S. Wilkinson, F. Schmidt, M. Hüben, E. Weinhold and N. O. Reich, *Bioconjugate Chem.*, 2008, **19**, 476–479; (*c*) S. Kim, A. Gottfried, R. R. Lin, T. Dertinger, A. S. Kim, S. Chung, R. A. Colyer, E. Weinhold, S. Weiss and Y. Ebenstein, Enzymatically Incorporated Genomic Tags for Optical Mapping of DNA–Binding Proteins, *Angew. Chem., Int. Ed.*, 2012, **51**, 3578–3581; (*d*) G. M. Hanz, B. Jung, A. Giesbertz, M. Juhasz and E. Weinhold, Sequence-specific labeling of nucleic acids and proteins with methyltransferases and cofactor analogues, *J. Visualized Exp.*, 2014, **93**, e52014.

13 S. M. Douglas, A. M. Marblestone, S. Teerapittayanon, A. Vazquez, G. M. Church and W. M. Shih, Rapid prototyping of 3D DNA-origami shapes with caDNAno, *Nucleic Acids Res.*, 2009, **37**, 5001–5006.

14 K. Goedecke, M. Pignot, R. S. Goody, A. J. Scheidig and E. Weinhold, Structure of the N6-adenine DNA methyltransferase M•TaqI in complex with DNA and a cofactor analog, *Nat. Struct. Biol.*, 2001, **8**, 121–125.

15 J. V. Jokerst and J. T. McDevitt, Programmable nano-bio-chips: multifunctional clinical tools for use at the point-of-care, *Nanomedicine*, 2010, **5**, 143–155.
16 S. Carrara, Nano-bio-technology and sensing chips: new systems for detection in personalized therapies and cell biology, *Sensors*, 2010, **10**, 526–543.
17 Q. Zhang, Q. Jiang, N. Li, L. Dai, Q. Liu, L. Song, J. Wang, Y. Li, J. Tian, B. Ding and Y. Du, DNA Origami as an In Vivo Drug Delivery Vehicle for Cancer Therapy, *ACS Nano*, 2014, **8**, 6633–6643.
18 H. Pues, N. Bleimling, B. Holz, J. Wölcke and E. Weinhold, Functional Roles of the Conserved Aromatic Amino Acid Residues at Position 108 (Motif IV) and Position 196 (Motif VIII) in Base Flipping and Catalysis by the N6-Adenine DNA Methyltransferase from Thermus aquaticus, *Biochemistry*, 1999, **38**, 1426–1434.